JOURNAL OF MATERIALS SCIENCE 21 (1986) 3615–3624

Various atmosphere effects on sintering of compacts of SiO_2 microspheres

T. Y. TSENG, J. J. YU
Institute of Electronics, College of Engineering, National Chiao Tung University, Hsinchu, Taiwan

The densification behaviour of highly ordered SiO_2 compacts sintered at 1000° C in H_2O (g) + N_2, static air, N_2 and 5% HCl + N_2 atmospheres was investigated. Densification rate was found to be atmosphere dependent. Surface tension to viscosity ratios were obtained for various sintering atmospheres using available sintering models. Scanning electron microscopy observations were employed to describe the different stages in the sintering of ordered compacts and to show the effects of various atmospheres on the microstructural development of ordered compacts.

1. Introduction

It has been shown that a gaseous atmosphere might change the viscosity and surface tension of a glass, therefore, the densification of glass powder compacts could be affected by the atmosphere. Cutler [1] reported that the densification of soda–lime glass powder compacts is sensitively affected by the water vapour partial pressure of the ambient atmosphere. Water vapour at high partial pressures has a greater effect than at low partial pressures. Water vapour appears to decrease the viscosity without significantly affecting the surface tension at high partial pressures. At low partial pressures, water vapour decreases both the surface tension and the viscosity of the soda–lime glass, thus the rate of shrinkage was insensitive to low water vapour partial pressures. The surface tension of a commercial soda–lime–silica glass was measured in various atmospheres in the temperature range 450 to 700° C [2]. All gases having linear and non-polar molecules have virtually no effect on the surface tension of soda–lime–silica glass. This was found to be the case with dry air, dry nitrogen, helium and hydrogen. Gases having polar molecules, such as water vapour, sulphur dioxide, ammonia and hydrogen chloride, lower the surface tension of soda–lime–silica glass by varying amounts. The surface tension of soda–lime–silica glass was found to decrease nearly proportional to the square root of the water vapour partial pressure. For fused silica, water vapour showed no significant effect on the surface tension from 1100 to 1300° C. This indicates that no adsorption from a water vapour atmosphere will take place on the oxygen surface of fused silica in this temperature range.

In a previous study [3], the sintering behaviour of highly ordered powder compacts formed from spherical, nearly monosized SiO_2 particles was investigated. The densification results indicated that sintering of ordered compacts could be divided into several stages which was supported by the agreement between experimental results and calculated linear shrinkage values. Rearrangement and the differential micro-densification process, which produce regions with larger pores and lower shrinkage rates, have occurred during the sintering of most of the irregularly packed particles [4–6], but have been minimized in ordered compacts. These results demonstrated that the highly ordered compacts would be the best candidate for quantitative sintering studies. However, the sintering study was only carried out in static air and did not consider the effect of atmosphere on the sintering of ordered compacts. The purpose of this investigation is to show the effects of various atmospheres including H_2O (g), N_2, air, HCl (g) on the sintering behaviour of highly ordered SiO_2 powder compacts. Microstructural evolution is followed by scanning electron microscopy observations for 1000° C isothermal sintering in various atmospheres and is correlated to sintering process.

2. Experimental procedure

2.1. Preparation of materials

Spherical hydrous silica particles with a narrow size distribution were produced by the reactions of tetraethylorthosilicate (TEOS) (Merck Art. 800658, West Germany) in reagent grade ethanol of concentrated ($\approx$ 30 wt % NH_3) ammonia [7, 8]. Green bodies were formed by allowing particles in the as-prepared well-dispersed solution to settle slowly (about 2 months) by gravitational force. After complete settling, the residual solution was drawn off and the subsequent ambient drying led to cracking of the precipitated cake into several large pieces. The irregularly shaped broken compacts were carefully removed from the flask and cut to dimensions of about 1 mm (thickness) × 40 mm^2 (area) for sintering. All powder compacts were dried for 24 h at 200° C and then calcined for 1 h at 500° C prior to sintering to remove residual bound water [8]. Scanning electron microscope (SEM) (Hitachi S-570, Hitachi Ltd, Tokyo) and transmission electron microscope (TEM) (Hitachi H-600, Hitachi Ltd, Tokyo) were used to characterize powders and powder compacts. Powder true density was measured

0022–2461/86 $03.00 + .12

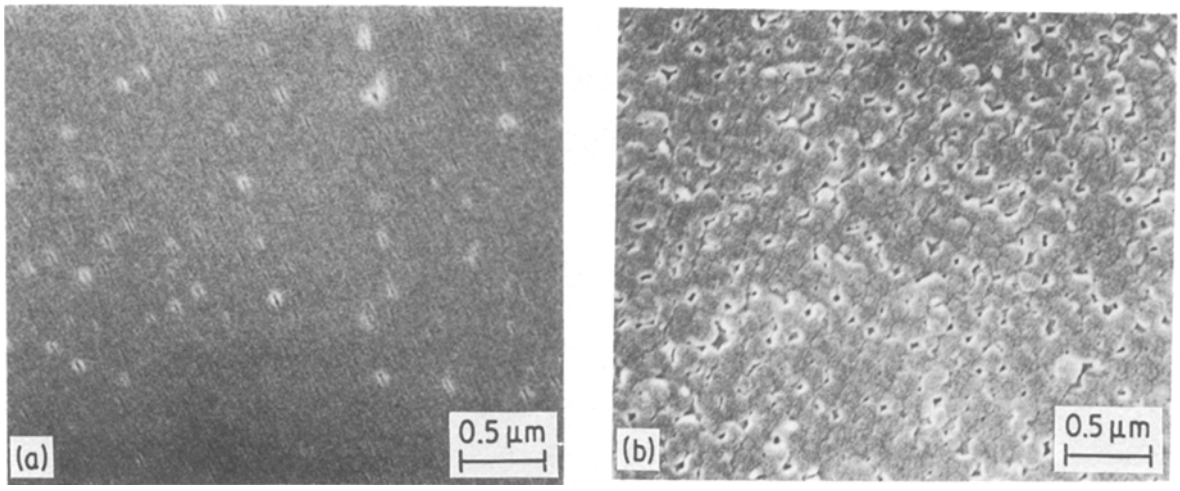

Figure 1 Scanning electron micrographs of sintered compacts with 84% relative density for (a) as-polished and (b) well-etched sample surfaces.

using a helium gas pycnometer (Model SPY-2, Quantachrome Corp., Syosset, New York).

2.2. Sintering in various atmospheres

A three zone furnace (Model MB-71, Thermco Products Corp., Orange, California) with fused silica tube (of diameter 5 in.) was used for sintering. During the experiments, the temperature was accurately maintained at 1000 $\pm$ 1° C. The SiO_2 compacts were isothermally sintered under various atmospheres for various time periods. For sintering in the nitrogen atmosphere, the atmosphere surrounding the particle compacts was maintained by nitrogen flowing through the furnace tube at the rate of 5 litre min^{-1}. For sintering in the H_2O (g) atmosphere, water vapour was generated by boiling distilled water in a sealed flask and was carried into the furnace tube by nitrogen gas at the same flow rate. For sintering in the HCl (g) atmosphere, 50 ml HCl gas was carried into the fused silica furnace tube (of diameter 2 in.) by 1 litre N_2/min^{-1}. The compacts were also sintered in a static air atmosphere as well as an atmosphere of 20% oxygen plus 80% nitrogen. A purifier was used to remove moisture in the nitrogen and oxygen gases before they flowed into the furnace tube.

Bulk densities of sintered compacts were determined by the displacement method using deionized water. Per cent relative density (ϱ_R) was calculated from bulk density and true density measurements. Powder X-ray diffraction (XRD) patterns were obtained with a diffractometer (Model XC-60, Toshiba, Yokohama, Japan) using nickel-filtered Cu$K\alpha$ radiation. Microstructural development was observed by SEM. Prior to the observations by SEM, the sintered samples were deliberately ground, polished and cleaned. In a selective etching system, the ion-beam thinning system (Edwards, IBT-200, Manor Royal, Crawley, Sussex, UK) was used to reveal the true microstructure by bombardment of high energy (6 keV) noble gas ions (Ar^+) on the sample surface. The milling time ranged from 5 to 30 min depended on the extent of sintering. Fig. 1a shows the polished surface of a sintered sample with 84% relative density (3 h in air atmosphere). The microstructure was obscured by the polishing procedure. A suitable etching process revealed the microstructure clearly as shown in Fig. 1b.

3. Results and discussion

3.1. Powder and green compact characterization

TEM (Fig. 2) shows that the diameter of the silica particle is about 0.18 μm; XRD analysis (Fig. 3) indicates that the SiO_2 powders are amorphous. The true density of the powders was measured to be 2.21 g cm^{-3} after calcination at 1000° C for 5 h in a static air atmosphere.

Green bodies, prepared by particle sedimentation from well-dispersed suspensions, contain a regular arrangement of spherical particles. The scanning electron micrographs (Figs 4a and b) show the two-dimensional arrangement of the spheres; the particles arrange themselves in either "hexagonal closed-packed

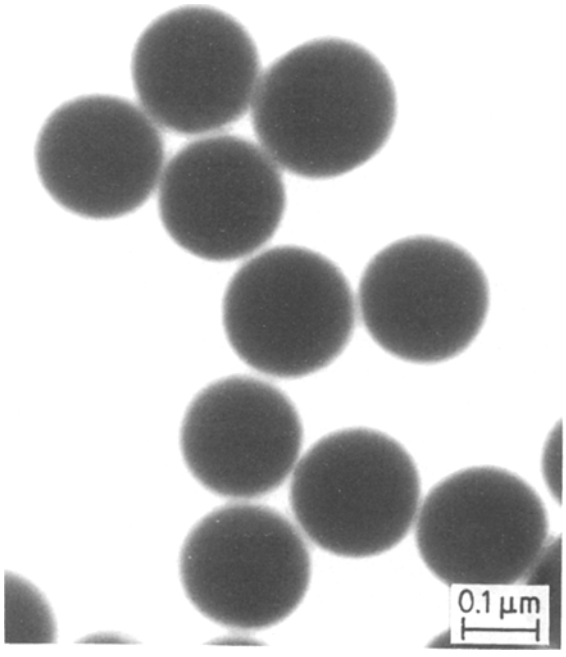

Figure 2 Transmission electron micrograph of SiO_2 particles.

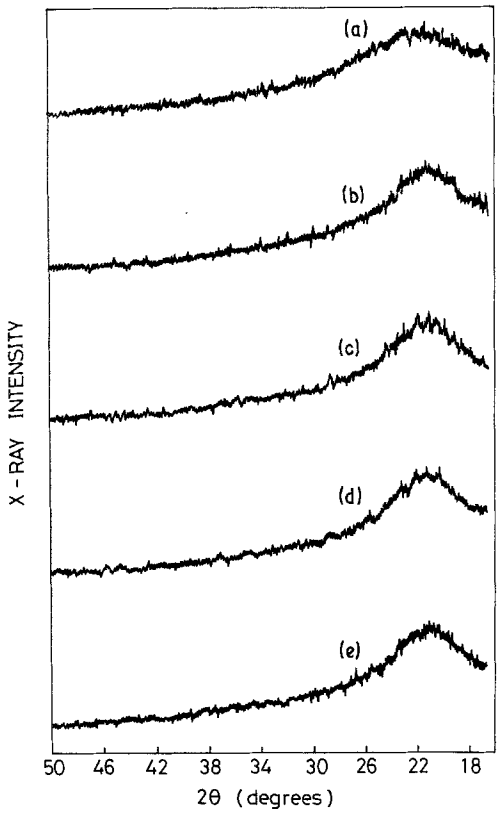

Figure 3 XRD patterns for silica compacts sintered in the following conditions: (a) 500° C, 1 h, in static air, (b) 1000° C, 3 h, in H_2O (g) + N_2, (c) 1000° C, 24 h, in static air, (d) 1000° C, 96 h, in N_2, (e) 1000° C, 25 h, in HCl (g) + N_2.

planes" or "cubic planes". These planes stack layer by layer to construct the three-dimensional structure of the compact. In several areas (note arrow in Fig. 4a), it is evident that hexagonal close-packed planes stack directly on top of each other to form a "simple hexagonal structure". This "simple" hexagonal structure has been reported in previous studies [8, 9]. Two types of pore channels in this order structure model compact would be formed:

1. three-particle (3p) channels in "hexagonal close-packed planes", the calculated channel radius is ≈ 16 nm (for 0.18 μm particle size);
2. four-particle (4p) pore channels in "cubic planes", the calculated channel radius is ≈ 41 nm.

The average green density of the real compacts (for 20 samples) was measured to be 60 $\pm$ 1% theoretical density (2.21 g cm^{-3}), close to the theoretical density of the simple hexagonal close-packed structure (60.46%). This value is considerably below the value of 74% for three-dimensional close-packed structure. It seems unlikely that packing defects (e.g. vacancies, grain boundaries, etc.) account for the entire difference. This suggests that lower density packing structures (e.g. "simple" hexagonal, body-centred cubic, etc.) are important in these compacts [8].

3.2. Influence of atmosphere on sintering

Fig. 5 shows the different densification rates of the silica powder compacts in various atmospheres. The compacts sintered in H_2O (g) + N_2 atmosphere reached $\approx 100\%$ relative density and became translucent in less than 90 min, while the compacts sintered in a static air atmosphere took about 11 h and that sintered in the N_2 atmosphere took about 100 h to reach the same relative density. Within this experiment, the compacts sintered in 5% HCl (g) + N_2 atmosphere for 25 h were still porous. The relative density was only 68%; this indicates that the HCl gas inhibited densification of model SiO_2 compacts in the present study. The scanning electron micrograph in Fig. 6a shows the polished surface of the compact sintered at 1000° C for 5 h in H_2O (g) + N_2 atmosphere. Only randomly located pores, which correspond to vacancies and voids, were found in the photomicrograph. The regular pore array has completely closed. The polished surface of the compact sintered in static air atmosphere contained closed pores (Fig. 6b). It is difficult to identify the individual particles due to the neck growth at the contact of particles and centre to centre approach of the spheres.

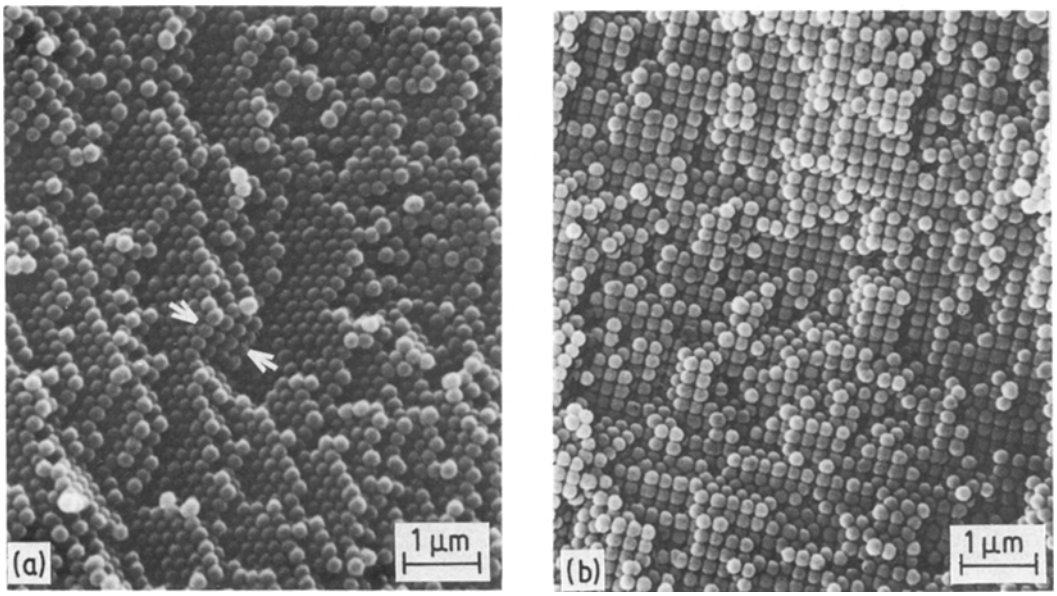

Figure 4 (a, b) Scanning electron micrographs for fracture surfaces of model green compacts.

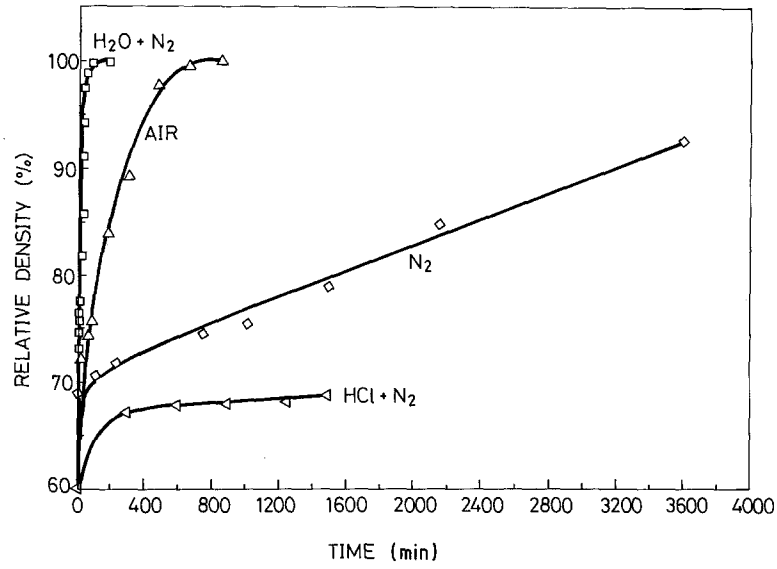

Figure 5 Plots of relative density against sintering time in various atmospheres.

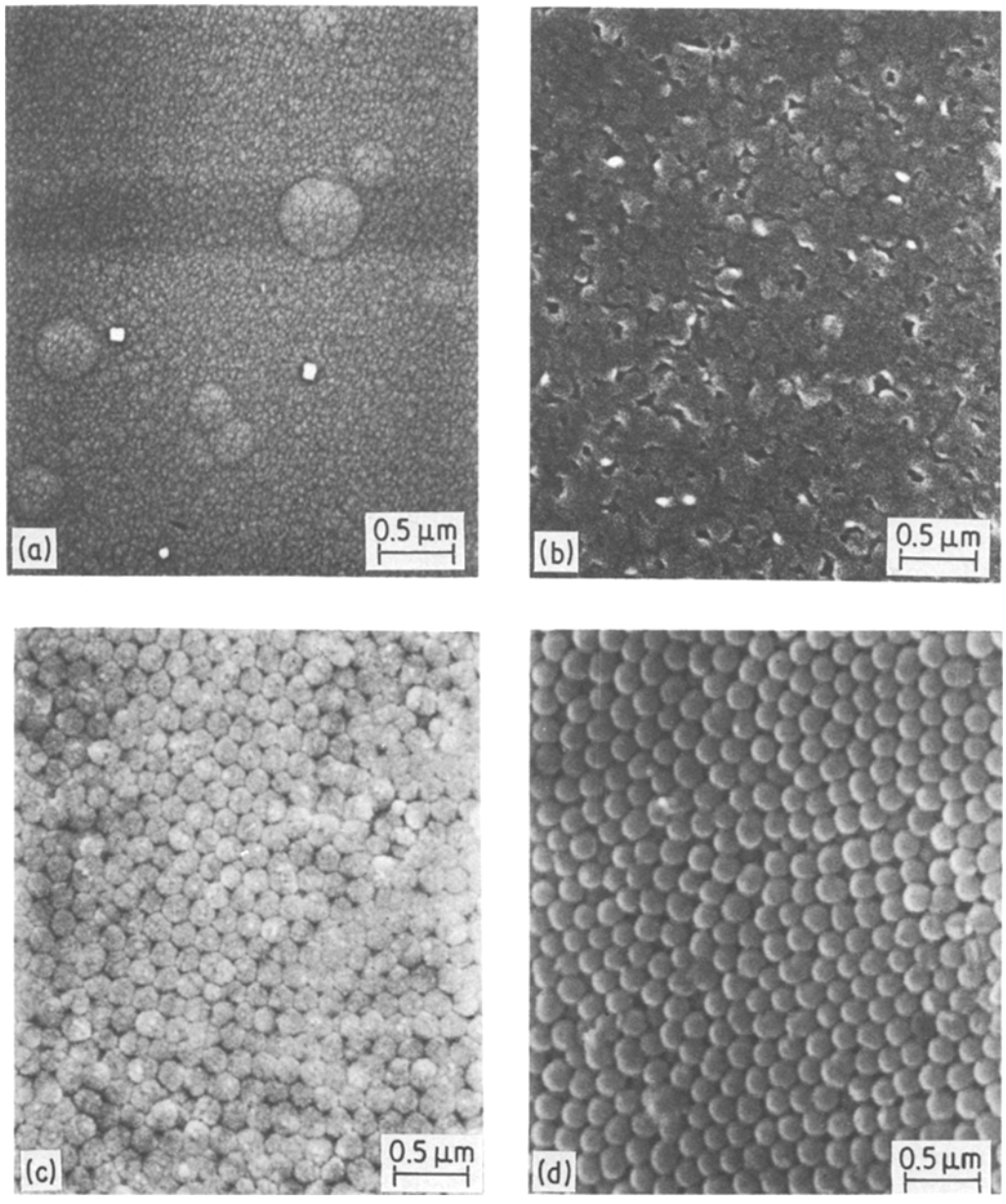

Figure 6 Scanning electron micrographs for the well-etched sample surfaces after sintering for 5 h in (a) H_2O (g) + N_2, (b) static air, (c) N_2 and (d) HCl (g) + N_2 atmospheres.

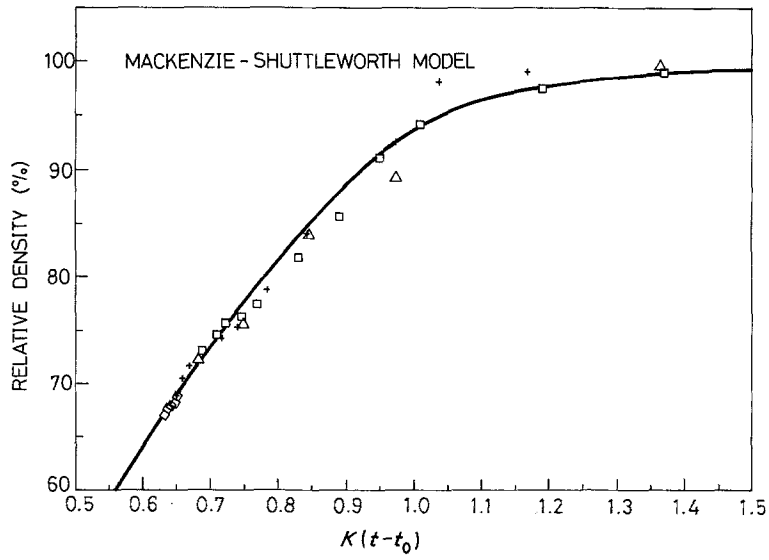

Figure 7 Fit of experimental sintering data to the Mackenzie–Shuttleworth model. Atmosphere: □, $H_2O + N_2$; △, air; +, N_2; ◇, HCL + N_2.

The compacts in N_2 and HCl (g) + N_2 atmospheres sintered slightly so that the individual particles were still distinct (Figs 6c and d). The neck growth and centre to centre approach phenomena were not obvious.

According to the experiments of Wagstaff *et al.* [10, 11], water vapour acts as a source of oxygen or weakens the glass structure through the formation of hydroxyl groups. It thus increases the rate of crystallization of stoichiometric SiO_2 and vitreous silica. But the XRD pattern (Fig. 3) shows that the SiO_2 powder sintered in H_2O (g) or another atmosphere was still amorphous (even after they have reached 100% theoretical density). The phase transformation of SiO_2 powders did not contribute to the various densification rates in this study.

The sintering of glass was suggested [12, 13] to be by a viscous flow mechanism. The rate of linear shrinkage is proportional to the surface tension and inversely proportional to the viscosity of the material. The rate of linear shrinkage, $\Delta L/L_0$ is defined as

$$\Delta L/L_0 = 3\gamma t/8\eta R \quad (1)$$

where γ is the surface energy, η the viscosity, t the sintering time and R the particle radius. Two other models are the Mackenzie and Shuttleworth [14] and Scherer [15] models which both provide relationships between relative density and reduced time of sintering. The Mackenzie–Shuttleworth model considered the shrinkage in a structure composed of isolated closed pores while the Scherer model considered the shrinkage of a cubic array of cylindrical particles. The sintering kinetics were analysed in terms of these two models. The solid line in Fig. 7 shows the predicted variation of the relative density, ϱ_R against reduced time, $K(t - t_0)$, based on the Mackenzie–Shuttleworth model. For the reduced time, t_0 is a fictitious time at which ϱ_R equalled zero and K is described by

$$K = \gamma n^{1/3}/\eta \quad (2)$$

where n, the number of pores per unit volume of solid phase, can be given by [16]

$$n = \frac{P}{4\pi R^3/3} \quad (3)$$

where P is the number of pores per particle and R the particle radius. For the uniform microstructure used in this study, it is reasonable to estimate $P = 1$. Data are fit to the theory by plotting reduced times (from the theoretical curve in Fig. 7) against sintering times

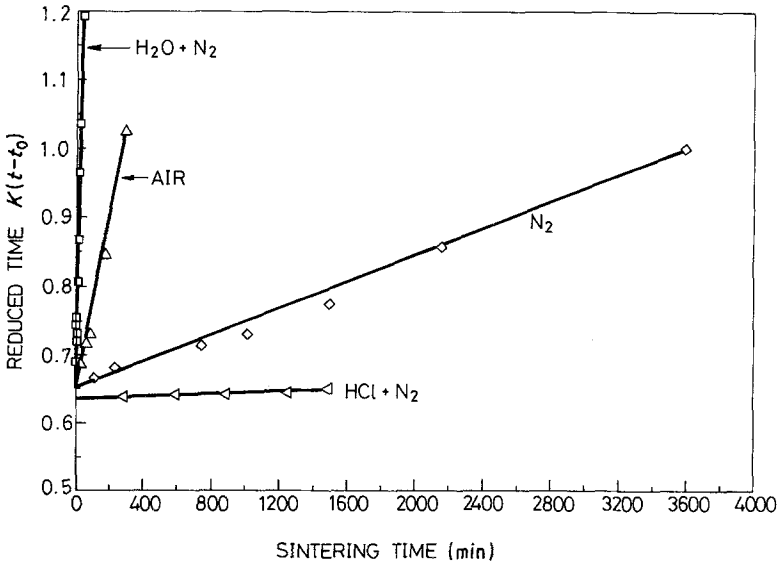

Figure 8 Plots of reduced time against sintering time for the Mackenzie–Shuttleworth model.

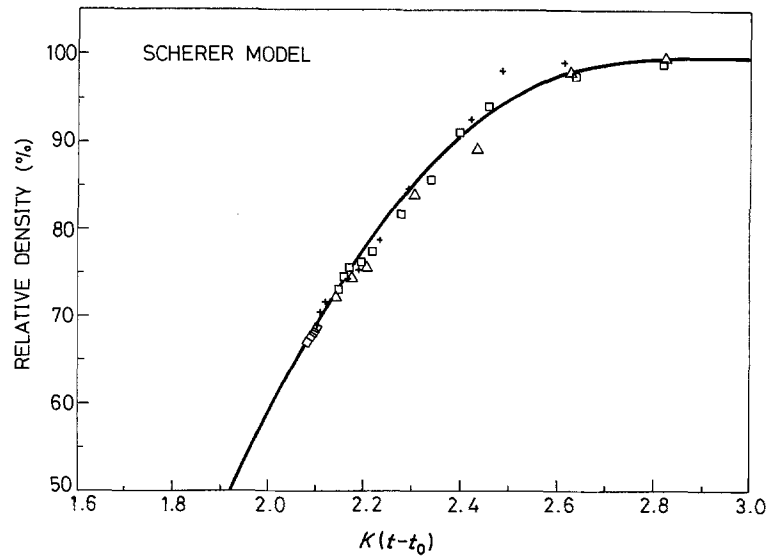

Figure 9 Fit of experimental sintering data to the Scherer model. Atmosphere: □, $H_2O + N_2$; △, air; +, N_2; ◇, $HCl + N_2$.

corresponding to the experimentally measured densities. These plots should be straight lines with slope K. The values of K from the slopes of the lines in Fig. 8 are listed in Table I. The experimental data show a good fit to the theoretical curve (Fig. 7). Using Equation 2, values for surface tension to viscosity ratio can be calculated for each sintering atmosphere (Table I).

As in the Mackenzie–Shuttleworth model, Scherer provided a theoretical relationship between the relative density and the reduced time (shown by the solid line in Fig. 9). In this case

$$K = (\gamma/\eta l_0)(\varrho_s/\varrho_0)^{1/3} \quad (4)$$

where γ is the surface energy, η the viscosity, l_0 the parameter related to pore size, ϱ_s the theoretical density of the solid and ϱ_0 the initial compact density prior to sintering. Experimental data were fit to the Scherer model ($\varrho_s = 2.21\,g\,cm^{-3}$ and l_0 was taken to be twice the particle radius) and the values of K were determined from the slopes of the lines in Fig. 10 in the same way as described for the Mackenzie–Shuttleworth model. The proportional constant, K, and surface tension to viscosity ratio, γ/η in various atmospheres are listed in Table I. It has been shown that both the surface energy and the viscosity of silica depend on the sintering atmosphere; thus the absolute value cannot be derived from K, only their ratio, γ/η, can be determined. For sintering silica glass in a static air atmosphere, the surface energy, γ, was reported to be $2.8 \times 10^{-5}\,J\,cm^{-2}$ ($280\,erg\,cm^{-2}$). The viscosity in static air is thus calculated to be $1.07 \times 10^{11}\,Pa\,sec^{-1}$, agreeing with Sacks and Tseng's result ($\approx 9 \times 10^{10}\,Pa\,sec^{-1}$). However, the calculated viscosity is considerably lower than that derived by Johnson *et al.* [17] and Scherer [18]. Moisture in the air atmosphere would be the most likely effect of lowering the viscosity because the experiments of Scherer and Johnson *et al.* were performed in dry helium atmosphere.

Several papers [1, 19, 20] which reported the reactions between water vapour and silica glass, have been published. They suggested that water molecule dissociated on entry and produced two hydroxyl groups in the atomic network of the glass according to the following equation:

$$\text{–Si–O–Si–} + H_2O \rightarrow 2\left(\text{–Si–OH}\right) \quad (5)$$

The rupture of the silicon–oxygen–silicon bridge and consequent weakening of the structure will decrease

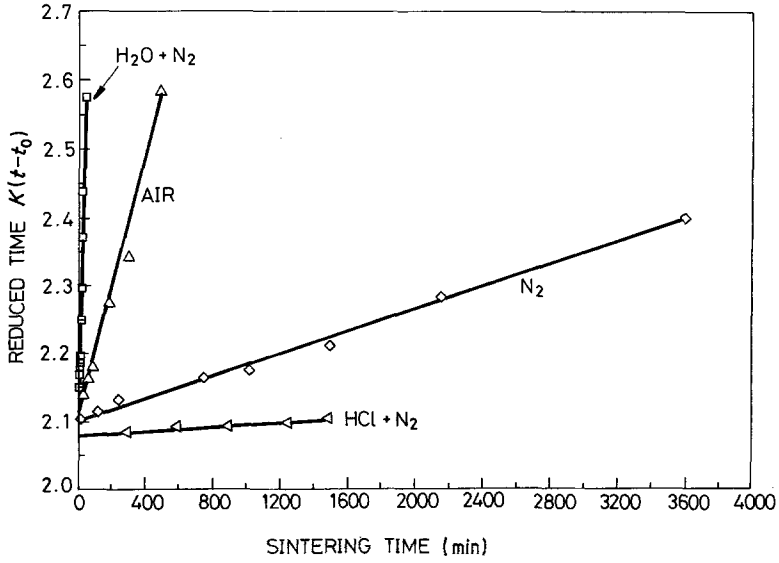

Figure 10 Plots of reduced time against sintering time for the Scherer model.

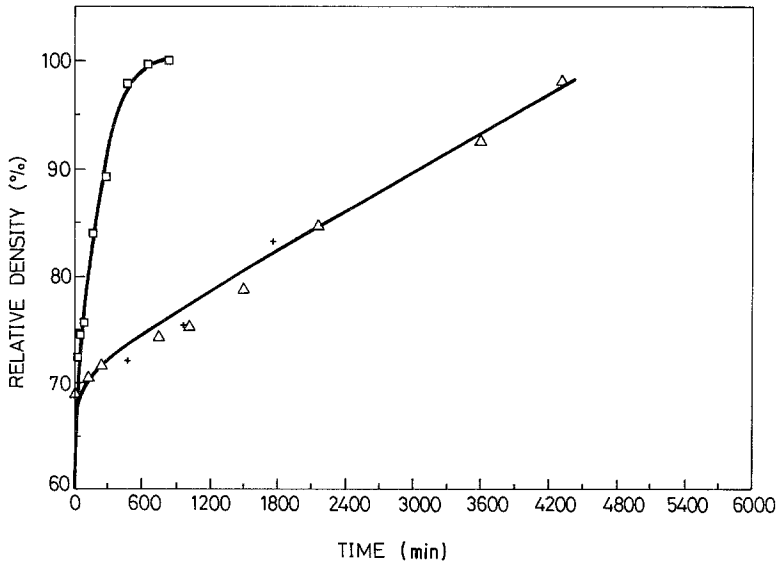

Figure 11 Plots of relative density against sintering time in (△) N_2 (+) 20% O_2 + 80% N_2, and (□) static air atmospheres.

both the viscosity and the surface tension of the glass. Cutler [1] confirmed this phenomenon at low partial pressure of water vapour (< 20 mm Hg). He also suggested that the surface tension became constant at high water vapour partial pressures while the viscosity continued to decrease proportional to the square root of the water vapour partial pressure. Parikh [2] showed that non-polar gases, such as dry air, nitrogen, hydrogen and helium, had very little influence on the surface tension of the soda–lime–silica glass, whereas polar gases, such as water vapour, sulphur dioxide, ammonia, and hydrogen chloride, lowered the surface tension by varying amounts. He also showed that surface tension was decreased in proportion to the square root of the water vapour partial pressure. Although his data did not go beyond a partial pressure of 16 mm Hg water vapour, it is obvious that increasing the water vapour partial pressure cannot continue to decrease the surface tension since negative values of surface tension will be reached. Although it was difficult to determine quantitatively the water vapour partial pressure in the present experiment, it is reasonable to expect high partial water vapour pressure in H_2O (g) + N_2 atmosphere since large quantities of steam were continuously carried into the furnace tube. We can conclude that the more rapid densification rate of the model SiO_2 compacts sintered in H_2O (g) + N_2 than in N_2 atmosphere is due to much lower viscosity and slightly lower surface tension of the silica powder in the presence of water vapour.

SiO_2 compacts in static air densified more rapidly than in N_2 atmosphere. The reason is investigated below: air consists of ≈80% N_2, ≈20% O_2, some amount of water vapour (moisture), and a very small amount of gases such as CO_2, H_2 and noble gases. CO_2, H_2 and noble gases will have little effect on the densification rate because of their negligible quantities in air. Either water varpour or O_2 contributed to the larger densification rate. To determine which one is dominant, the SiO_2 compacts were also sintered in an atmosphere with 20% O_2 and 80% N_2. The moisture in the N_2 and O_2 gases was removed by a purifier before they entered the furnace tube. The densification rate was shown (Fig. 11) to be nearly equal to that in N_2 atmosphere. Thus we can conclude that water vapour (moisture) played a major role in the air atmosphere in enhancing the sintering of SiO_2 powder compacts.

Elmor [21] suggested that HCl gas reacted with silanol group or siloxane bridges according to the following equations:

$$\text{–Si–OH} + \text{HCl} \rightarrow \text{–Si–Cl} + \text{H}_2\text{O} \qquad (6)$$

$$\text{–Si}\!\!>\!\!\text{O}\!\!<\!\!\text{Si–} + 2\,\text{HCl} \rightarrow 2\,\text{–Si–Cl} + \text{H}_2\text{O} \qquad (7)$$

However, substitution of Cl^- ions in the glass at OH^- sites does not decrease the glass viscosity, because chloride ions are more tightly bonded than silanols. The surface tension of the soda–lime–silica glass was reported [2] to decrease in the presence of hydrogen chloride (probably by the formation of dipoles). Therefore, the slower densification rate of SiO_2 powder compacts sintered in the 5% HCl (g) + N_2 atmosphere than in the N_2 atmosphere was probably due to the lower surface tension of SiO_2 powders.

Coble [22] suggested that the final density of the

TABLE I Reduced time proportional constant, K, and surface tension to viscosity ratio, γ/η, in various atmospheres

Sintering atmospheres	K (sec^{-1})			γ/η ($cm\,sec^{-1}$)
	(M–S)	(Scherer)	(Average)	
H_2O (g) + N_2	2.1×10^{-4}	2.02×10^{-4}	2.06×10^{-4}	3.0×10^{-9}
Static air	2.0×10^{-5}	1.6×10^{-5}	1.8×10^{-5}	2.6×10^{-10}
N_2	1.6×10^{-6}	1.4×10^{-6}	1.5×10^{-6}	2.2×10^{-11}
HCl (g) + N_2	2×10^{-7}	3×10^{-7}	2.5×10^{-7}	3.6×10^{-12}

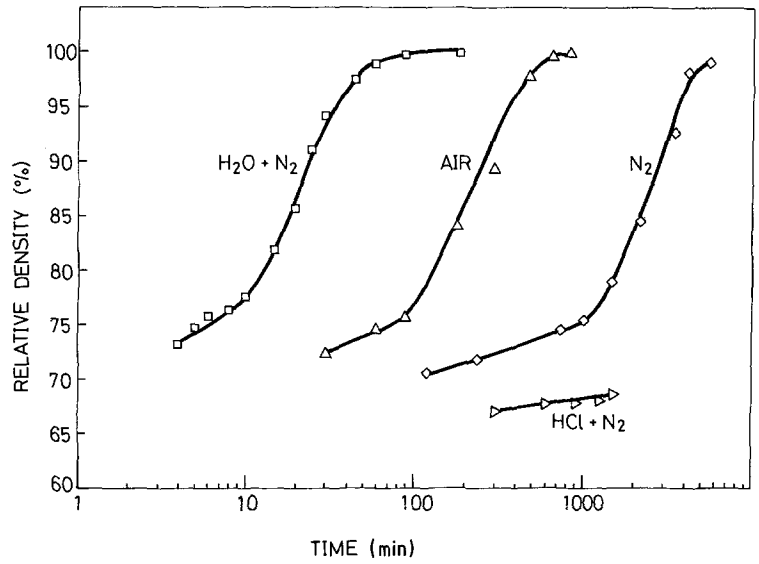

Figure 12 Plots of relative density against logarithm of sintering time for atmospheres indicated.

glass was limited by the diffusion speed of the sintering atmosphere. That is, at an advanced stage of sintering, the open pore channels are pinched off at the specimen surface first, and the trapped gas in the closed pores cannot escape to the outside atmosphere. The gas enclosed is compressed as further shrinkage proceeds. When the internal gas pressure counterbalances the surface tension driving force, shrinkage stops. The limiting densities that can be reached depend on the diffusivity of the gas in the solid. At low gas diffusivity, the sealed pores shrink to their respective stable size and a low final density is obtained. At relatively high gas diffusivity, the final shrinkage is not impeded by the presence of the gas and a high final density is obtained. At intermediate gas diffusivity, the kinetics of gas diffusion to the surface control the rate of final pore shrinkage. However, nearly 100% relative density and translucency could be attained for sintering in H_2O (g), static air and N_2 atmospheres. This indicates that the final densities were not limited by the above three atmospheres for the model compacts used in the present experiment. Sintering of compacts in HCl (g) + N_2 atmosphere persisted only for 25 h. Data on the final density were not available. Nothing can be said about the limiting final density in the HCl (g) atmosphere.

Plots of relative density against logarithm of sintering time are shown in Fig. 12 for various sintering atmospheres. In each plot (except in the HCl atmosphere), and upward break is observed at approximately the same relative density (≈ 75 to $\approx 77\%$). The results indicate that the densification process may be divided into at least two stages. Similar results were found in earlier experiments [3, 4]. In Sacks and Pask's experiments, compacts of different states of agglomeration were sintered. In the first stage of sintering, the smaller particles in close-packed regions densified quickly, and by their "pulling away", larger pores "opened up". After the small pores closed, the subsequent densification of larger pores corresponded to a higher stage of sintering. Sacks and Tseng [3] sintered the SiO_2 model compacts in air atmospheres for

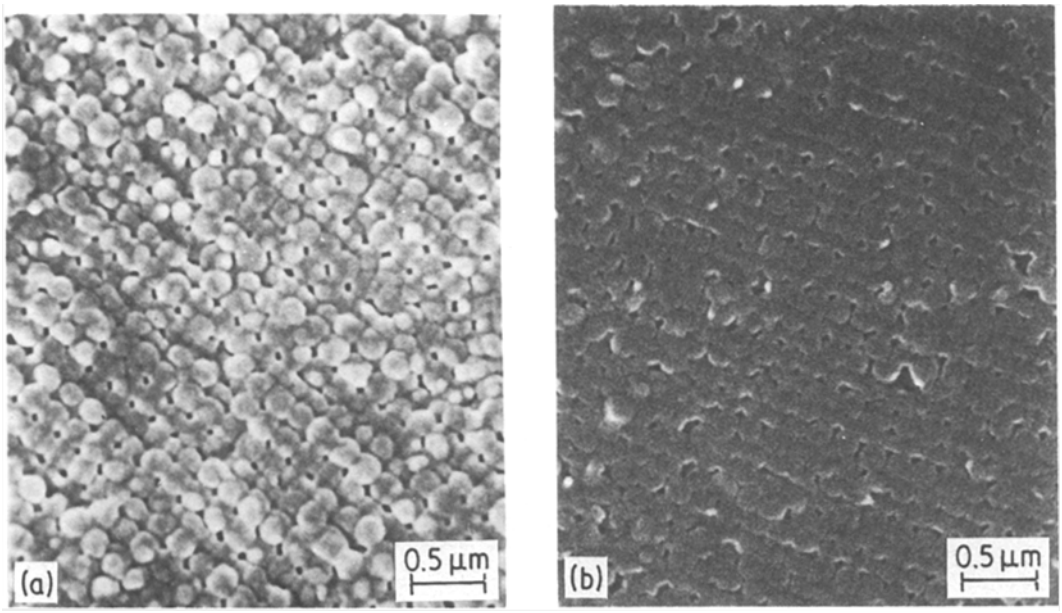

Figure 13 Scanning electron micrographs of sintered samples with (a) 79% and (b) 82% relative densities.

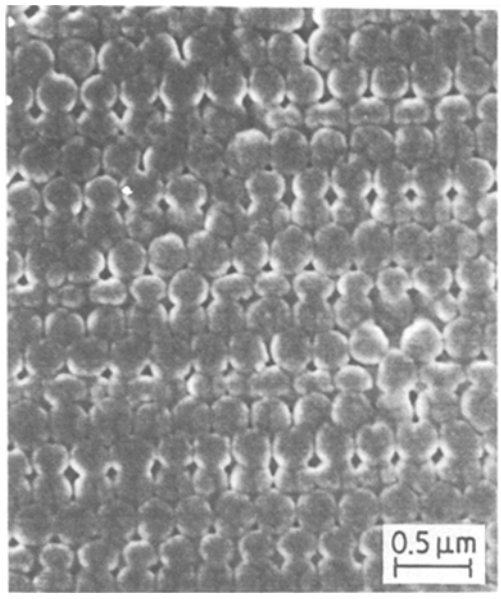

Figure 14 Scanning electron micrograph for polished surface of sintered compact of particles $\approx 0.28\,\mu m$ diameter with 76% relative density.

900, 950, 1000 and 1050° C. An upward break was found at approximately the same relative density (≈ 72 to $\approx 73\%$) in the plots of relative density against logarithm of sintering time. With the aid of mercury porosimetry, they suggested that shrinkage of 3p pore channels was the dominant process responsible for densification during the first linear region, whereas the second linear region was primarily associated with the shrinkage of 4p pore channels.

SEM observations (Figs 13 and 14) also support the preceding interpretation for the upward break observed in each plot of Fig. 12 for various atmospheres. Fig. 13 shows the scanning electron micrographs of the samples with different ϱ_R values (≈ 79 and $\approx 82\%$). Most of the 3p pore channels have already closed during the first stage, while those remaining are generally quite small. In contrast, many 4p pore channels, considerably larger in size, are evident in Figs 13a and b. To elucidate this phenomenon more clearly, model compacts with larger SiO_2 spherical particles ($\approx 0.28\,\mu m$) were prepared and sintered in static air. A better resolution scanning electron micrograph (Fig. 14) was obtained and shows the same shrinkage sequence as shown in Fig. 13. These results agree with Sacks and Tseng's observations [3]. So it is reasonable to associate the first linear region with the shrinkage of the smaller pores (i.e. the 3p pore channels), while the shrinkage of 4p pore channels is associated with the second linear region.

The densification rate of the model compacts in static air atmosphere in this study was compared with Sacks and Tseng's result [3]. The particle packing condition was similar and the green density was nearly the same ($\approx 60\%$), whereas the particle size was different in the two experiments. In Sacks and Tseng's experiment, the particle size was $\approx 0.5\,\mu m$, considerably larger than that of the present study ($\approx 0.18\,\mu m$). Compacts with larger particle sizes were shown (Fig. 15) to have a lower densification rate. According to the Mackenzie–Shuttleworth model, the densification rate is proportional to K (equal to $\gamma/\eta R(3P/4\pi)^{1/3}$) and hence it is inversely proportional to particle radius. The proportional relation is not found in the present comparison because the moisture content in the sintering atmosphere was unknown.

In the bulk of the hexagonal close-packed structure, the co-ordination number of each particle is 12. However, each particle in the hexagonal close-packed surface layer contacts at most with nine other particles. Therefore, surface tension (the driving force of sintering) of the surface layer is less than that of the bulk. Densification in the surface layer is thus expected to be less than the bulk. Fig. 16 confirms this phenomenon. After sintering for 45 min in H_2O (g) + N_2 atmosphere, the bulk was almost completely densified (Fig. 16a), whereas the surface layer was slightly sintered (Fig. 16b).

4. Conclusions

The SiO_2 model compacts were prepared and sintered at 1000° C in the following atmospheres: (1) H_2O (g) + N_2, (2) static air, (3) dry N_2 and (4) 5% HCl (g) + N_2 (in sequence of densification rate, from high to low). Water vapour decreased both the viscosity

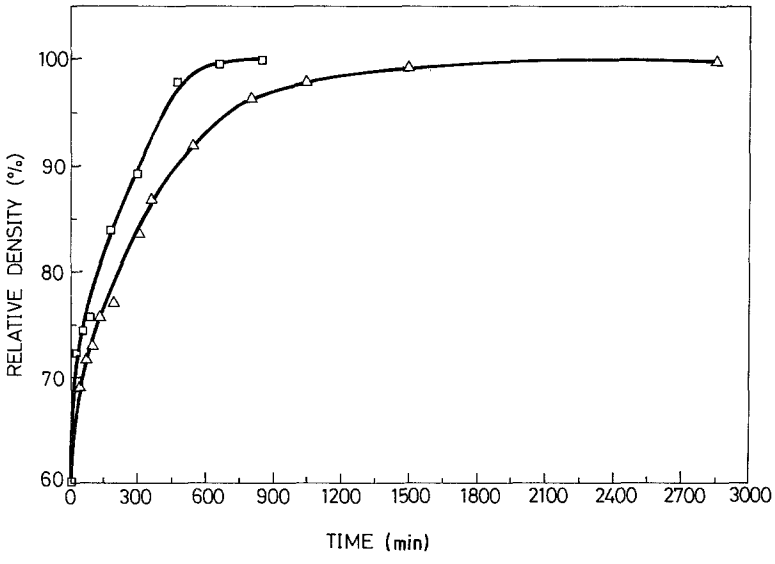

Figure 15 Plots of relative density against sintering time in static air for model compacts of different particle sizes: □, $0.18\,\mu m$; △, $0.5\,\mu m$.

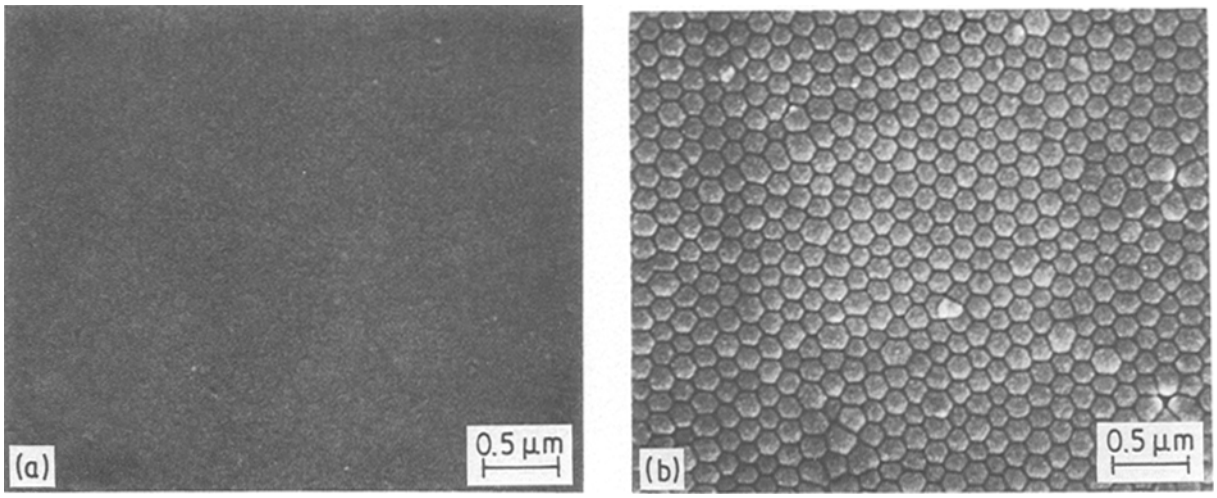

Figure 16 Scanning electron micrographs for (a) fracture surface and (b) top surface of sintered compacts with ≈ 100% relative density.

and the surface tension of SiO_2 powders by formation of silanol groups in the powder surface. The enhanced densification indicated that the viscosity of SiO_2 was reduced more than the surface tension. Oxygen gas was found to have no influence on the densification rate; this indicated that moisture dominated the densification of the SiO_2 compact in the static air atmosphere. HCl gas was found to inhibit sintering of the SiO_2 compact by decreasing the surface tension.

Densification kinetics were fit to the Mackenzie–Shuttleworth and Scherer models. Various values of K, the proportional constant in these models, were found in various sintering atmospheres. Since both surface tension and viscosity were sensitive to sintering atmosphere, it is not possible to clearly delineate the effect of atmosphere on viscosity and surface tension separately in the present study; only their ratios can be determined.

An ion-thinning system was used to selectively etch the polished surfaces of sintered compacts. Microstructure evolutions were clearly observed by SEM. Densification and SEM observation results indicate sintering of ordered compacts can be divided into several stages.

References

1. I. B. CUTLER, *J. Amer. Ceram. Soc.* **52** (1969) 11.
2. N. M. PARIKH, *ibid.* **41** (1958) 18.
3. M. D. SACKS and T. Y. TSENG, *ibid.* **67** (1984) 532.
4. M. D. SACKS and J. A. PASK, *ibid.* **65** (1982) 70.
5. H. E. EXNER and G. PETZOW, in "Sintering and Catalysis", edited by G. C. Kuczynski (Plenum, New York, 1975) p. 279.
6. H. E. EXNER, G. PETZOW and P. WELLNER, in "Sintering and Related Phenomena", edited by G. C. Kuczynski (Plenum, New York, 1973) p. 351.
7. W. STOBER, A. FINK and E. BOHN, *J. Colloid Interface Sci.* **26** (1968) 62.
8. M. D. SACKS and T. Y. TSENG, *J. Amer. Ceram. Soc.* **67** (1984) 526.
9. R. L. HOFFMAN, *Trans. Soc. Rheol.* **16** (1972) 155.
10. F. E. WAGSTAFF, S. D. BROWN and I. B. CUTLER, *Phys. Chem. Glasses* **5** (1964) 76.
11. F. E. WAGSTAFF and K. J. RICHARDS, *J. Amer. Ceram. Soc.* **49** (1966) 118.
12. J. FRENKEL, *J. Phys. (USSR)* **9** (1945) 385.
13. G. C. KUZYNSKI, *J. Appl. Phys.* **20** (1949) 116.
14. J. K. MACKENZIE and R. SHUTTLEWORTH, *Proc. Phys. Soc. (Lond.) Sect. B* **62** (1949) 833.
15. G. W. SCHERER, *J. Amer. Ceram. Soc.* **60** (1977) 236.
16. *Idem, ibid.* **67** (1984) 709.
17. D. W. JOHNSON Jr, E. M. RABINOVICH, J. B. MACCHESNEY and E. M. VOGEL, *ibid.* **66** (1983) 688.
18. G. W. SCHERER, *ibid.* **60** (1977) 239.
19. A. J. MOULSON and J. P. ROBERTS, *Trans. Faraday Soc.* **57** (1960) 1208.
20. B. A. MORROW and I. A. CODY, *J. Phys. Chem.* **80** (1976) 1998.
21. T. H. ELMOR, *J. Amer. Ceram. Soc.* **64** (1981) 150.
22. R. L. COBLE, *ibid.* **45** (1962) 123.

Received 19 August
and accepted 19 December 1985